Understanding the glass-forming ability of $Cu_{50}Zr_{50}$ alloys in terms of a metastable eutectic

W.H. Wang[a)]
Institute of Physics, Chinese Academy of Sciences, Beijing 100080, People's Republic of China

J.J. Lewandowski
Department of Materials Science and Engineering, Case Western Reserve University, Cleveland, Ohio 44106

A.L. Greer
Department of Materials Science and Metallurgy, University of Cambridge, Cambridge CB2 3QZ, United Kingdom

(Received 17 October 2004; accepted 3 March 2005)

Interest in finding binary alloys that can form bulk metallic glasses has stimulated recent work on the Cu–Zr system, which is known to show glass formation over a wide composition range. This work focuses on copper mold casting of $Cu_{50}Zr_{50}$ (at.%), and it is shown that fully amorphous rods up to 2-mm diameter can be obtained. The primary intermetallic phase competing with glass formation on cooling is identified, and the glass-forming ability is interpreted in terms of a metastable eutectic involving this phase. Minor additions of aluminum increase the glass-forming ability: with addition of 4 at.% Al to $Cu_{50}Zr_{50}$, rods of at least 5-mm diameter can be cast fully amorphous. The improvement of glass-forming ability is related to suppression of the primary intermetallic phase.

I. INTRODUCTION

There has been much interest in finding a binary alloy composition capable of forming a bulk metallic glass (BMG), i.e., of forming a glass with a minimum dimension greater than 1 mm. If a BMG were found with a true binary or near-binary composition, it would facilitate fundamental analysis of glass formation; in particular, atomistic modeling would be much easier than it would be for the multicomponent systems usually considered necessary for BMG formation. Also, any binary BMG would be an excellent starting point for the development of multicomponent systems giving still better glass-forming ability (GFA).

The search for a binary BMG has recently focused on the Cu–Zr system. From early work, it is known that by melt-spinning $Cu_{100-x}Zr_x$ (at.%), metallic glasses can be obtained in an unusually wide composition range of $x =$ 25 to 60 at.%.[1] The origins of such comparatively good GFA have been extensively discussed.[2–7] An atomic radius difference of more than 10% is important for glass formation,[8,9] and Cu–Zr meets this criterion (Goldschmidt radii: Cu, 0.128 nm; Zr, 0.161 nm). The size difference leads to copper being an anomalous fast diffuser in zirconium[10] but zirconium being a slow diffuser in copper. Good GFA is also associated with a negative heat of mixing, and Cu–Zr shows a particularly large value of –23 kJ mol^{-1}.[11] The diffusional asymmetry and the negative heat of mixing are favorable for forming amorphous Cu–Zr by mechanical alloying[12] and by the solid-state amorphization reaction.[13]

Looking for BMG formation, Xu et al.[14] studied $Cu_{100-x}Zr_x$ alloys in the composition range $x = 34$ to 40 at.%. They reported that at the best glass-forming composition in this range, $Cu_{64}Zr_{36}$, 2 mm rods can be cast completely amorphous. In related work, a similar GFA has been reported for $Cu_{46}Zr_{54}$.[15] Inoue et al.[16] studied Cu–Zr in the range 30–70 at.% Zr, and reported that the best glass-forming composition is $Cu_{60}Zr_{40}$, at which 1.5 mm rods can be cast completely amorphous. Wang et al.[17] independently studied the same composition range as Xu et al.[14] and concluded that there is a very narrow composition range (width <1 at.%) for good GFA. They estimated the optimum glass-forming composition to be $Cu_{64.5}Zr_{35.5}$. They associated good GFA with eutectics but noted that their best GFA did not coincide with a deep eutectic in the equilibrium phase diagram. Tang et al.[18] studied GFA in the $Cu_{100-x}Zr_x$ system for $x = 40$ to 55 at.% and found that $Cu_{50}Zr_{50}$ rods could be cast completely amorphous with diameters up to 2 mm.

a)Address all correspondence to this author.
e-mail: whw@aphy.iphy.ac.cn
DOI: 10.1557/JMR.2005.0302

There has also been interest in enhancing the GFA of Cu–Zr by minor additions of other elements. Inoue et al.[19] showed that $Cu_{46}Zr_{47}Al_7$ can be cast fully amorphous up to 3 mm in diameter. This system has been further studied by Xu et al.[15] through addition of yttrium: $Cu_{46}Zr_{47-y}Al_7Y_y$; with $y = 5$ at.% the GFA is maximized and rods up to 100-mm diameter can be cast fully amorphous. The enhancement of the GFA of Cu–Zr through addition of aluminum and other elements was interpreted in terms of the heats of mixing between the alloy components.[15]

The often-cited three empirical rules for BMG formation[7] include criteria based on atomic sizes and heats of mixing as mentioned above but first state that the alloy should have more than three components. Although binary Cu–Zr appears capable of BMG formation, the system is clearly distinct from a typical multicomponent BMG. Liquids of Cu–Zr have been characterized in terms of Angell's strong/fragile classification.[20] The fragility index m, estimated by heating a Cu–Zr metallic glass at 20 K min^{-1}, is 62 which is significantly higher than the values of 30–40 normally associated with multicomponent BMGs[21–23] and identifies the binary liquid as fragile.

While there is some understanding of why binary Cu–Zr shows glass-forming ability over a wide composition range, much remains to be done, in particular to more clearly delineate BMG formation. The present work focuses on studying the GFA near the composition $Cu_{50}Zr_{50}$ (at.%). Cooling on the margin of glass formation and x-ray diffraction with in situ annealing are used to identify the crystalline phases, which are the main competitors to glass formation on cooling. These phases are then used to interpret the GFA in terms of eutectics, including a metastable eutectic.

II. EXPERIMENTAL

Ingots of $Cu_{50}Zr_{50}$ (nominal composition, at.%) were prepared by arc-melting copper and zirconium (each 99.9 at.% purity) in a Ti-gettered argon atmosphere. Ingots of $(Cu_{50}Zr_{50})_{100-x}Al_x$ ($x = 0$, 2, 4, and 6) alloys were prepared by arc-melting $Cu_{50}Zr_{50}$ ingots with aluminum (99.99 at.%) under the same conditions. Ingots were then remelted and suction-cast into a copper mold to obtain cylindrical rods 50 mm long. To obtain different cooling rates, rods were cast with diameters from 1 to 5 mm.

Structural characterization was by mounting rod cross-sections for x-ray diffractometry (XRD) with Cu K_α radiation. The as-cast rods were studied on an MAC M03 XHF diffractometer (Japan). Changes in structure on annealing were studied in situ in a Siemens D500 high-temperature diffractometer under nitrogen atmosphere. The diffraction patterns were collected by step-scanning with a step-length of 0.05°, and the collecting time at each point was 5 s. Samples were subjected to a sequence of 30-min anneals at successively higher temperatures. To calibrate the diffraction peaks, polycrystalline Si powder was added on the sample for the purpose of calibration. The accuracy of Bragg-angle determination permitted by this internal calibration is essential for reliable identification of the crystalline phases. Differential scanning calorimetry (DSC) was carried out in a Perkin Elmer DSC-7 (USA) at a heating rate of 20 K min^{-1}. Melting of the samples was studied by differential thermal analysis (DTA) using a Perkin Elmer DTA-7 at a heating rate of 10 K min^{-1}.

III. RESULTS

Rods of $Cu_{50}Zr_{50}$ were cast with different diameters to measure glass-forming ability. As shown by XRD of rod cross-sections (Fig. 1), samples with diameter $d \leqslant 2$ mm are fully amorphous, while those with $d \geqslant 3$ mm are partially crystalline. The full amorphicity of 2 mm diameter samples was further checked by transmission electron microscopy (TEM), including high-resolution imaging and selected-area diffraction; apart from isolated 1–2 nm particles (less than 5% in overall volume fraction), there was no evidence of crystallinity. For a 1-mm-diameter sample, high-resolution TEM shows only the uniform contrast expected for a single glassy phase.

As noted by Lin and Johnson,[24] the maximum d for which samples are fully amorphous can be used to estimate the critical cooling rate R_c, according to

$$R_c\ (\mathrm{K\ s^{-1}}) = \frac{10}{\{d\ (\mathrm{cm})\}^2} \quad . \tag{1}$$

Using Eq. (1), R_c for $Cu_{50}Zr_{50}$ is estimated to be ~250 K s^{-1}. With addition of aluminum to this alloy, the glass-forming ability is clearly increased. With 4 at.% Al, fully amorphous rods are obtained even at 5 mm, the maximum diameter tested. For $(Cu_{50}Zr_{50})_{96}Al_4$ the estimate of R_c from Eq. (1) is $\leqslant$40 K s^{-1}.

Examination of samples that are not fully amorphous is useful in identifying the crystalline phases that are competitors to glass formation during casting. Even for this simple binary Cu–Zr alloy, there is a complex phase formation sequence during solidification. The phases giving rise to the Bragg peaks in Fig. 1 are identified as far as possible. The key phase identification is that of $Cu_{51}Zr_{14}$, based on a match with the data in the Power diffraction file 42-1185 [Powder Diffraction Data, International Center for Diffraction Data, published by JCPDS, Pennsylvania, 2000] as set out in Table I. The peak positions fit the standard diffraction data well, especially in the 2θ range 30–60°. The relative intensities do not match so well, presumably because there is

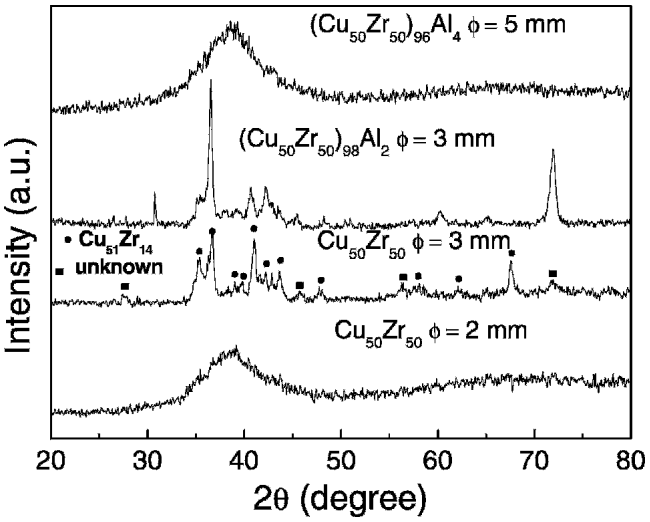

FIG. 1. X-ray diffractograms of as-cast rods of $Cu_{50}Zr_{50}$ and $(Cu_{50}Zr_{50})_{100-x}Al_x$ (at.%). The diameters of the rods are indicated and the phases giving rise to the Bragg peaks are identified as far as possible.

TABLE I. The positions and relative intensities of Bragg peaks of the as-cast $Cu_{50}Zr_{50}$ alloy with a diameter of 3 mm (shown in Fig. 1) measured in the present work, compared with Powder Diffraction File 42-1185 [Powder Diffraction Data, International Center for Diffraction Data, published by JCPDS, Pennsylvania, 2000], to identify the phase $Cu_{51}Zr_{14}$.

	2θ (degrees)		Relative intensity		
(*hkl*)	File	Measured	File	Measured	Note
(202)	28.30	28.50	2	3	
(302)	35.17	35.25	2	70	Superposed on Zr(002)
(400)	36.935	36.93	10	100	Superposed on Zr(101)
(222)	38.683	38.71	6	8	
(312)	39.863	39.80	34	12	
(213)	40.875	40.90	65	80	
(321)	41.873	41.70	17	30	
(410)	42.565	42.45	100	55	
(303)	43.010	43.00	22	35	
(411)	43.983	43.95	42	45	
(223)	46.156	45.95	23	15	
(412)	48.173	48.00	8	20	
(430)	57.548	57.50	8	10	
(432)	62.163	62.19	3	5	
(441)	67.625	67.60	7	50	

preferred orientation of the phase and because of overlap with peaks from other phases. It is clear, however, that the main phase is $Cu_{51}Zr_{14}$ and not the expected CuZr matching most closely the composition of the glass. Surprisingly, the system favors the more complex structure $Cu_{51}Zr_{14}$ with a composition significantly different from the glass.

As shown in Fig. 1, in $Cu_{50}Zr_{50}$ there are also other unidentified competing phases. It can also be seen from Fig. 1 that when aluminum is added to the alloy, the main crystalline phase is changed. From the observed peaks it is not possible to identify the additional phase, and we designate it "unidentified."

Figure 2 shows DSC curves for the as-cast $Cu_{50}Zr_{50}$ and $(Cu_{50}Zr_{50})_{94}Al_6$ BMGs. Each alloy has a distinct glass transition at T_g and a sharp crystallization onset at T_x, further confirming the glassy structure of the alloys. Larger values of the reduced glass transition temperature T_{rg} ($= T_g/T_l$,[25] where T_l is the liquidus temperature of the alloy) or of the temperature range of the supercooled liquid ΔT ($= T_x - T_g$) are expected to indicate better glass-forming ability. With 6 at.% addition of Al to $Cu_{50}Zr_{50}$, T_{rg} increases from 0.55 to 0.60, and ΔT from 47 to 69 K. The increase in glass-forming ability on addition of aluminium is accompanied by a substantial increase in thermal stability of the glass: T_x is increased from 717 to 770 K. Figure 3 shows DTA curves obtained on melting the $Cu_{50}Zr_{50}$ and $(Cu_{50}Zr_{50})_{94}Al_6$ BMGs as well as the $Cu_{50}Zr_{50}$ BMG pre-annealed for ~4 h above T_x (~800 K). There are some differences, not significant, between the melting behaviors of the as-cast and the annealed $Cu_{50}Zr_{50}$ BMG, the latter presumably having a phase constitution close to equilibrium. In each case, there is a wide melting range, showing that these compositions do not undergo simple eutectic melting. This is in contrast to many BMGs, which form at the compositions of deep eutectics.

The effects of annealing the BMGs were studied using in situ XRD. This technique has the advantages that its good time resolution can permit the detection of intermediate stages of crystallization, which might otherwise be missed. The results of a series of isothermal 30-min anneals of the same $Cu_{50}Zr_{50}$ BMG (2 mm diameter) are shown in Fig. 4. (The Si diffraction peaks are from the polycrystalline Si powder for calibration.) As noted

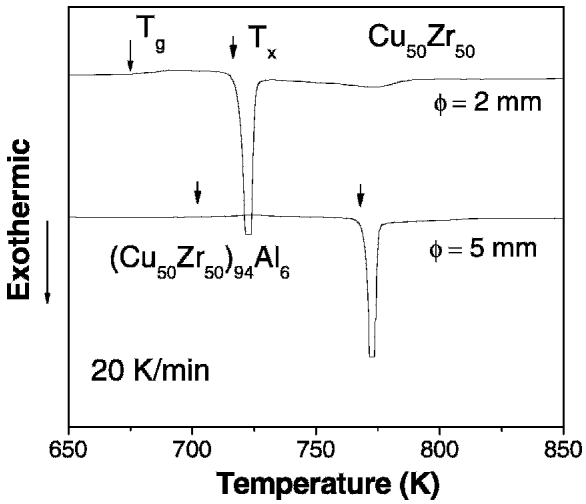

FIG. 2. Differential scanning calorimetry traces of the as-cast rods of $Cu_{50}Zr_{50}$ and $(Cu_{50}Zr_{50})_{94}Al_6$ alloys. The temperatures of the glass transition T_g and of crystallization onset T_x are arrowed.

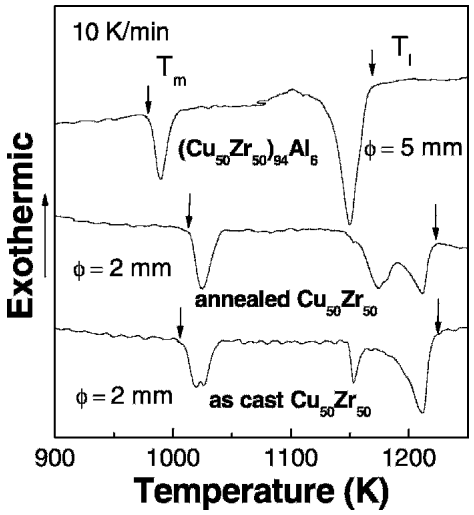

FIG. 3. Differential thermal analysis traces of as-cast rods of $Cu_{50}Zr_{50}$ and $(Cu_{50}Zr_{50})_{94}Al_6$ BMGs as well as the $Cu_{50}Zr_{50}$ BMG pre-annealed for ~4 h above T_x (~800 K), showing the temperature range of melting.

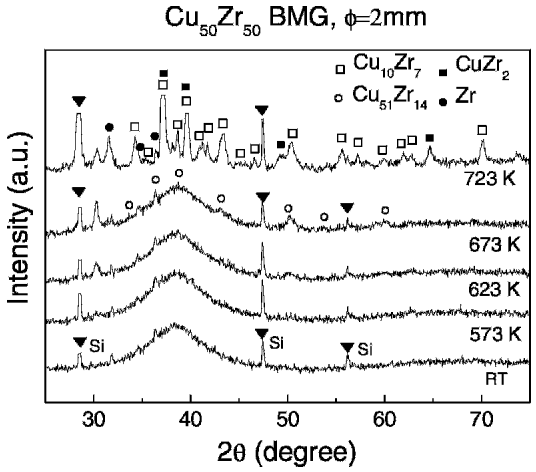

FIG. 4. X-ray diffractograms of a 2-mm-diameter cast rod of $Cu_{50}Zr_{50}$ during in situ annealing. The as-cast rod is fully amorphous. A sequence of anneals is performed, with 30 min at each of the temperatures shown. The Bragg peaks for silicon arise from the polycrystalline powder added for calibration.

above, high-resolution TEM (HRTEM) shows some isolated 1–2-nm particles, ~5% in volume fraction. The corresponding crystalline phase(s) cannot be detected by continuous-scanning XRD in Fig. 1, but they become detectable by step-scanning XRD. Even in the as-cast rod (labeled RT in Fig. 4) there are two weak crystalline peaks (between 30° and 40°), which are above the amorphous background. Crystallization starts to become evident after the anneal at 673 K, which is just above T_g, in the supercooled liquid region. At this stage, the detectable phases are $Cu_{51}Zr_{14}$ and trace amounts of α–Zr. The $Cu_{51}Zr_{14}$ crystallites are of nanometer scale (~12 nm), as evidenced by the width of their diffraction maxima. At the higher annealing temperature of 723 K, just above T_x, the crystallization products are $Cu_{10}Zr_7$ and $CuZr_2$. Even after this heat treatment, there is still no evidence for the formation of the expected CuZr

Figure 5 shows the effects of annealing a 5 mm diameter sample of $Cu_{50}Zr_{50}$, which is not fully amorphous as-cast. The $Cu_{51}Zr_{14}$ phase when annealed at 723 K gives way to $Cu_{10}Zr_7$ and $CuZr_2$. The corresponding in situ XRD results for $(Cu_{50}Zr_{50})_{94}Al_6$ BMG (5-mm diameter) are shown in Fig. 6. For anneals at higher temperature, during which the sample becomes fully crystallized, the predominant phases are different from the crystallization products of the binary Cu–Zr BMG.

IV. DISCUSSION

The equilibrium phase diagram of Cu–Zr (Fig. 7), recently computed by Zeng et al.,[26] shows many eutectics depressing the liquidus far below the melting temperatures of the constituent elements, a feature associated with glass-forming ability. As noted above, the primary crystalline phase in $Cu_{50}Zr_{50}$, both on casting at the margin of glass formation and on annealing of the glass, is $Cu_{51}Zr_{14}$ (hexagonal, $P6/m$, a = 1.130 nm, c = 0.824 nm).[27] This phase is formed by solid-state reaction in Cu–Zr multilayers[28] and is the primary crystallization product in amorphous $Cu_{60}Zr_{20}Ti_{20}$.[27] It has the highest melting point of all the Cu–Zr intermetallics. It has also been observed that in ternary systems with copper and zirconium, e.g., Cu–Ti–Zr,[29] the $Cu_{51}Zr_{14}$ phase features in many invariant points, especially for copper-rich compositions.

Nevertheless, it is surprising that this phase is prominent for $Cu_{50}Zr_{50}$ alloys, since its composition is so rich

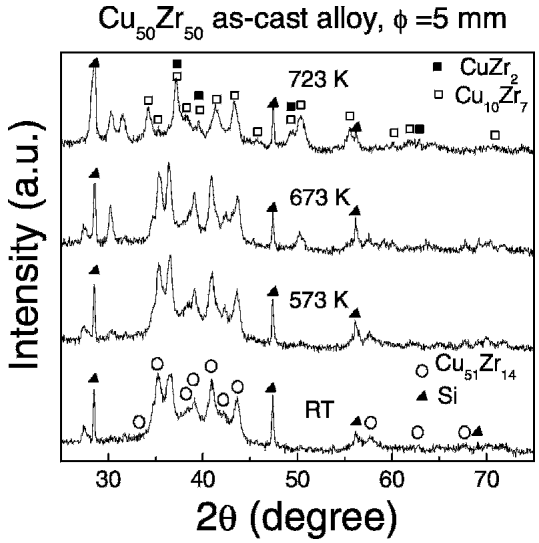

FIG. 5. X-ray diffractograms of a 5-mm-diameter cast rod of $Cu_{50}Zr_{50}$ during in situ annealing. The as-cast rod has $Cu_{51}Zr_{14}$ as its predominant crystalline phase. A sequence of anneals is performed, with 30 min at each of the temperatures shown.

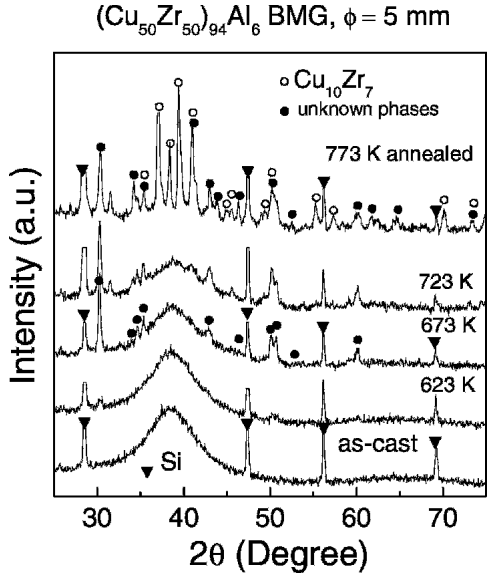

FIG. 6. X-ray diffractograms of a 5-mm-diameter cast rod of $(Cu_{50}Zr_{50})_{94}Al_6$ during in situ annealing. The as-cast rod is fully amorphous. A sequence of anneals is performed, with 30 min at each of the temperatures shown.

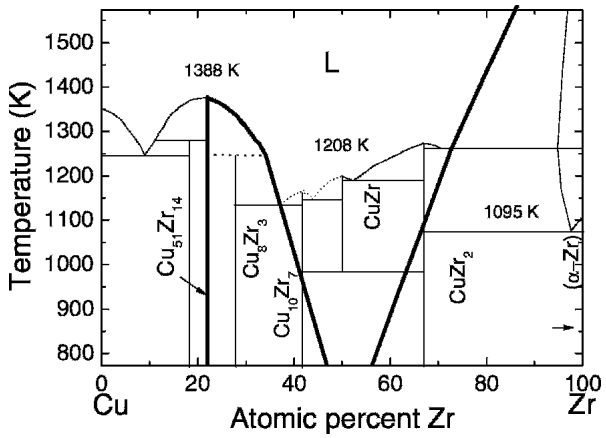

FIG. 7. The equilibrium phase diagram of Cu–Zr, according to the thermodynamic fitting by Zeng et al.[26] The bold lines indicate the extrapolated liquidus lines for the metastable eutectic of $Cu_{51}Zr_{14}$ and β–Zr. This eutectic is significant in the absence of the compounds $CuZr_2$, CuZr, $Cu_{10}Zr_7$, and Cu_8Zr_3.

in copper. On increasing the copper content around their best glass-forming composition of $Cu_{64.5}Zr_{35.5}$, Wang et al.[17] found that the primary phase changed from $Cu_{10}Zr_7$ to Cu_8Zr_3, the intermetallics closest to the alloy composition. For $Cu_{50}Zr_{50}$, the closest intermetallic is evidently CuZr; this has not been detected in the present work, even after annealing for 30 min at 723 K. In composition, the next closest intermetallics are $CuZr_2$ and $Cu_{10}Zr_7$, which are the phases seen on annealing at 723 K. Weihs et al.[28] claim that $Cu_{51}Zr_{14}$ is a metastable compound, but this is inconsistent with thermodynamic modeling of the Cu–Zr system.[26] In the present work, the disappearance of $Cu_{51}Zr_{14}$ on annealing results simply from its not being an equilibrium phase at an overall composition of $Cu_{50}Zr_{50}$. The apparent importance of $Cu_{51}Zr_{14}$ as a primary phase in the present work is difficult to explain but may reflect the influence of quenched-in nuclei, given the evidence for some nm-scale crystallites in the as-cast alloy.

That $Cu_{51}Zr_{14}$ is the primary phase of importance for analyzing glass formation shows it may be useful to consider metastable phase equilibria. The link between metastable eutectics and metallic glass formation was first explored by Highmore and Greer.[30] They showed that solid-state amorphization in systems such as Ni–Zr could be understood as eutectic melting in a metastable phase diagram. At the temperatures of reaction of polycrystalline nickel and zirconium in deposited multilayers, the intermetallic phases are initially unable to nucleate; the relevant phase diagram is then a very deep metastable eutectic between the terminal solid-solution phases. Systems showing solid-state amorphization, of which Ni–Zr and Cu–Zr are both examples, are characterized by a great asymmetry in their atomic diffusivities. The small late-transition-metal atoms (e.g., Ni in Ni–Zr) have interstitial-like diffusivities, orders of magnitude higher than those of the large early-transition metals (e.g., Zr in Ni–Zr). Fast diffusion of the late-transition metal permits mixing of the elements with slow diffusion of the early-transition metals inhibits the nucleation and growth of the equilibrium crystalline intermetallics.

In the present case, the relevant metastable phase diagram does not have all the compounds missing, but has $Cu_{51}Zr_{14}$ still present. The heavy lines sketched in Fig. 7 are extrapolations of equilibrium liquidus lines and show the metastable eutectic between $Cu_{51}Zr_{14}$ and β–Zr. Interestingly, this metastable eutectic is predicted to be in the composition range relevant for the good glass-forming ability seen at $Cu_{50}Zr_{50}$ and neighboring compositions. Wang et al. suggest displacement of best glass-forming compositions from eutectic compositions may be attributable to asymmetry in the coupled zone.[17] Here we point out that apparent displacement of glass-forming compositions can also result from the operation of metastable eutectics of the kind shown in Fig. 7. (We note in passing that yet other explanations of metallic glass formation displaced from eutectic compositions have been offered in terms of the difficulty of nucleating both crystalline phases.[31,32])

Even if a single deep metastable eutectic is relevant for glass formation, the intermetallic compounds whose absence gave rise to the metastable eutectic do eventually succeed in nucleating during heating of the alloy. By the time melting starts, the sample is likely to consist of a complex mixture of intermetallics not yet fully in equilibrium. The melting behavior seen for example in Fig. 3 can then be complex, and is not itself a good guide to glass formation.

The obviously improved glass-forming ability and thermal stability of the glass on addition of aluminum can be associated with destabilization of the $Cu_{51}Zr_{14}$ phase.[33–34] This appears to be the case, as shown by the data in Figs. 1 and 6.

V. CONCLUSIONS

The binary alloy $Cu_{50}Zr_{50}$ (at.%) can be cast fully amorphous in rods up to 2 mm in diameter. Casting larger-diameter rods on the margin of glass formation and annealing amorphous alloys show that the crystalline phase, which is the main competitor to glass formation in cooling, is $Cu_{51}Zr_{14}$, despite its enrichment in copper relative to the alloy composition. The glass-forming ability of $Cu_{50}Zr_{50}$ can be interpreted in terms of a deep metastable eutectic between $Cu_{51}Zr_{14}$ and β–Zr. This shows that the best glass-forming ability should be displaced from the eutectic compositions shown on the equilibrium phase diagram. Addition of aluminum to $Cu_{50}Zr_{50}$ greatly improves its glass-forming ability. With an addition of just 4 at.% Al, rods with diameters of at least 5 mm can be cast fully glassy. The addition of aluminum appears to destabilize $Cu_{51}Zr_{14}$ and thereby promote glass formation. The prospects are good for further development of BMGs based on minor alloying additions to $Cu_{50}Zr_{50}$.

ACKNOWLEDGMENTS

Support from the Natural Science Foundation of China, Grant No. 50321101 (for W.H.W.), the Reference Metals (for J.J.L.), and the European Commission (for A.L.G.) is gratefully acknowledged. The authors thank A. Moss, E. Marzbanrad, B. Yu, and M.B. Tang for experimental assistance and useful discussions.

REFERENCES

1. R. Ray, B.C. Giessen, and N.J. Grant: Formation of Cu–Zr metallic glasses. *Scripta Metall.* **2,** 359 (1968).
2. D. Turnbull: Under what conditions can a glass be formed? *Contemp. Phys.* **10,** 473 (1969).
3. W.L. Johnson: Thermodynamic and kinetic aspects of the crystal to glass transformation in metallic materials. *Prog. Mater. Sci.* **30,** 81 (1986).
4. A.L. Greer: Confusion by design. *Nature* **366,** 303 (1993).
5. A.L. Greer: Metallic glasses. *Science* **267,** 1947 (1995).
6. R.W. Cahn and A.L. Greer: Metastable states of alloys, in *Physical Metallurgy*, revised and enhanced edition, edited by R.W. Cahn and P. Haasen (Elsevier Sciences BV, Amsterdam, The Netherlands, 1996), Chap. 19.
7. A. Inoue: Stabilization of metallic supercooled liquid and bulk amorphous alloys. *Acta Mater.* **48,** 279 (2000).
8. T. Egami and Y. Waseda: Atomic size effect on the formability of metallic glasses. *J. Non-Cryst. Solids* **64,** 113 (1984).
9. D.B. Miracle, W.S. Sanders, and O.N. Senkov: The influence of efficient atomic packing on the constitution of metallic glasses. *Philos. Mag.* **83,** 2409 (2003).
10. A.D. Le Claire: Interdiffusion between Cu and Zr. *J. Nucl. Mater.* **69–70,** 70 (1978).
11. F.R. Boer, R. Boom, W.C.M. Matterns, A.R. Miedema, and A.K. Niessen: *Cohesion in Metals* (North-Holland, Amsterdam, The Netherlands, 1988).
12. E. Hellstern and L. Schultz: Amorphization of transition metal Zr alloys by mechanical alloying. *Appl. Phys. Lett.* **48,** 124 (1986).
13. M. Atzmon, J.R. Verhoeven, E.D. Gibson, and W.L. Johnson: Formation and growth of amorphous phases by solid-state reaction in elemental composites prepared by cold working. *Appl. Phys. Lett.* **45,** 1052 (1984).
14. D. Xu, B. Lohwongwatana, G. Duan, W.L. Johnson, and C. Garland: Bulk metallic glass formation in binary Cu-rich alloy series-$Cu_{100-x}Zr_x$ (x = 34, 36, 38.2, 40 at.%) and mechanical properties of bulk $Cu_{64}Zr_{36}$ glass. *Acta Mater.* **52,** 2621 (2004).
15. D. Xu, G. Duan, and W.L. Johnson: Unusual glass-forming ability of bulk amorphous alloys based on ordinary metal copper. *Phys. Rev. Lett.* **92,** 245504 (2004).
16. A. Inoue and W. Zhang: Formation, thermal stability and mechanical properties of Cu–Zr and Cu–Hf binary glassy alloy rods. *Mater. Trans.* **45,** 584 (2004).
17. D. Wang, Y. Li, B.B. Sun, M.L. Sui, K. Lu, and E. Ma: Bulk metallic glass formation in the binary Cu–Zr system. *Appl. Phys. Lett.* **84,** 4029 (2004).
18. M.B. Tang, D.Q. Zhao, M.X. Pan, and W.H. Wang: Binary Cu–Zr bulk metallic glasses. *Chin. Phys. Lett.* **21,** 901 (2004).
19. A. Inoue and W. Zhang: Formation, thermal stability and mechanical properties of Cu–Zr–Al bulk glassy alloys. *Mater. Trans.* **43,** 2921 (2002).
20. C.A. Angell: Formation of glasses from liquids and biopolymers. *Science* **267,** 1924 (1995).
21. D.N. Perera: Compilation of the fragility parameters for several glass-forming metallic alloys. *J. Phys. Condens. Matter* **11,** 3807 (1999).
22. J.M. Borrego, A. Conde, S. Roth, and J. Eckert: Glass-forming ability and soft magnetic properties of FeCoSiAlGaPCB amorphous alloys. *J. Appl. Phys.* **92,** 2073 (2002).
23. Z.F. Zhao and W.H. Wang: A highly glass-forming alloy with very low glass transition temperature. *Appl. Phys. Lett.* **82,** 4699 (2003).
24. X.H. Lin and W.L. Johnson: Formation of Ti–Zr–Cu–Ni bulk metallic glasses. *J. Appl. Phys.* **78,** 6514 (1995).
25. Z.P. Lu, H. Tan, Y. Li, and S.C. Ng: The correlation between reduced glass transition temperature and glass forming ability of bulk metallic glasses. *Scripta Mater.* **42,** 667 (2000).
26. K.J. Zeng, M. Hämäläinen, and H.L. Lukas: Phase diagram of Cu–Zr alloy. *J. Phase Equilibria* **15,** 577 (1994).
27. Á. Révész, A. Concustell, L.K. Varga, S. Suriñach, and M.D. Baró: Influence of the wheel speed on the thermal behaviour of $Cu_{60}Zr_{20}Ti_{20}$ alloys. *Mater. Sci. Eng. A* **375–377,** 776 (2004).
28. T.P. Weihs, T.W. Barbee, and M.A. Wall: Hardness, ductility, and thermal processing of Cu/Zr, and Cu/Cu–Zr nanoscale multilayer foils. *Acta Mater.* **45,** 2307 (1997).
29. R. Arroyave, T.W. Eagar, and L. Kaufman: Thermodynamic assessment of the Cu–Ti–Zr system. *J. Alloys Compd.* **351,** 158 (2003).

30. R.J. Highmore and A.L. Greer: Eutectics and the formation of amorphous alloys. *Nature* **339,** 363 (1989).
31. S. Bossuyt: Spatial localization of the nucleation rate and formation of inhomogeneous nanocrystalline dispersions in deeply undercooled glass forming liquids. *Scripta Mater.* **44,** 2781 (2001).
32. S. Bossuyt and A.L. Greer: Effects of positive feedback on crystallization kinetics and recalescence, in *Amorphous and Nanocrystalline Metals,* edited by R. Busch, T.C. Hufnagel, J. Eckert, A. Inoue, W.L. Johnson, and A.R. Yavari (Mater. Res. Soc. Symp. Proc. **806,** Warrendale, PA, 2004), p. 15.
33. Z.P. Lu and C.T. Liu: Role of minor alloying additions in formation of bulk metallic glasses: A Review. *J. Mater. Sci.* **39,** 3965 (2004).
34. W.H. Wang, Z. Bian, P. Wen, Y. Zhang, M.X. Pan, and D.Q. Zhao: Role of addition in formation and properties of Zr-based bulk metallic glasses. *Intermetallics* **10,** 1249 (2002).